

SODIUM/PROTON ANTIporter IN THE EURYHALINE CRAB *CARCINUS MAENAS*: MOLECULAR CLONING, EXPRESSION AND TISSUE DISTRIBUTION

DAVID W. TOWLE^{*,1,2}, MARY E. RUSHTON^{1,2}, DORIS HEIDYSCH^{1,2}, JASON J. MAGNANI¹,
MELANIE J. ROSE¹, ALICE AMSTUTZ², MARK K. JORDAN², DARCY W. SHEARER² AND WEN-SHU WU^{1,2}

¹Department of Biology, Lake Forest College, Lake Forest, IL 60045, USA and ²Mount Desert Island Biological Laboratory, Salsbury Cove, ME 04672, USA

Accepted 9 January 1997

Summary

Gill epithelial cells of euryhaline crustaceans demonstrate net inward transport of sodium ions, possibly via apical Na⁺/H⁺ antiporters, Na⁺/K⁺/2Cl⁻ cotransporters or Na⁺ channels working in series with the basolateral Na⁺+K⁺-ATPase. We have identified and sequenced the cDNA coding for a crustacean Na⁺/H⁺ antiporter, starting with mRNA isolated from gills of the euryhaline green shore crab *Carcinus maenas*. The complete 2595-base-pair cDNA includes an open reading frame coding for a 673-amino-acid protein. A search of GenBank revealed more than 20 high-scoring matches, all Na⁺/H⁺ antiporter sequences from mammalian, amphibian, teleost and nematode species. Injection of *Xenopus laevis* oocytes with cRNA transcribed from the cloned crab sequence substantially enhanced Na⁺-dependent H⁺ efflux from the oocytes. Analysis of crab tissue antiporter mRNA levels by

semi-quantitative reverse transcription–polymerase chain reaction revealed that posterior and anterior gills of *Carcinus maenas* expressed this antiporter the most strongly, followed in decreasing order by skeletal muscle, hepatopancreas, hypodermis and heart. Hydrophathy and transmembrane α -helix analysis suggested a 10-helix membrane-spanning topology of the antiporter protein. It is clear from this study that *Carcinus maenas* gills vigorously transcribe a gene coding for a Na⁺/H⁺ antiporter. Whether these gills also express a gene coding for an epithelial Na⁺ channel or Na⁺/K⁺/2Cl⁻ cotransporter remains to be demonstrated.

Key words: Na⁺/H⁺ antiporter, crab, gill, *Carcinus maenas*, molecular cloning, tissue distribution, cDNA sequence, Na⁺ transport, *Xenopus laevis* oocytes.

Introduction

The Na⁺/H⁺ antiporters, initially demonstrated in membrane vesicles prepared from mammalian kidney (Murer *et al.* 1976), play important roles in ionic homeostasis, acid–base balance, cell volume regulation and the response to growth-stimulating factors (reviewed by Counillon and Pouyssegur, 1993a; Bianchini and Pouyssegur, 1994). The four antiporter isoforms so far described in mammalian cells exhibit different tissue distributions and varying degrees of sensitivity to amiloride and its analogs but are all believed to be electroneutral, exchanging 1 Na⁺ for 1 H⁺ under most physiological conditions.

In contrast, a uniquely electrogenic Na⁺/H⁺ antiporter has been demonstrated in membrane vesicle preparations from crustacean tissues, including crab gill (*Carcinus maenas*; Shetlar and Towle, 1989), lobster hepatopancreas (*Homarus americanus*; Ahearn and Clay, 1989) and prawn hepatopancreas (*Macrobrachium rosenbergii* Ahearn *et al.* 1990). The crustacean antiporter appears to exchange 2 Na⁺ for 1 H⁺, resulting in a polarization of membrane potential (Shetlar and Towle, 1989). In the hepatopancreas, there is good evidence that the electrogenic antiporter is associated with the

apical membrane of epithelial cells (Ahearn *et al.* 1994). In addition to the well-characterized electrogenic Na⁺/H⁺ antiporter in crustacean epithelia, an electroneutral Na⁺/H⁺ antiporter was described recently in basolateral membrane vesicles from lobster (*Homarus americanus*) hepatopancreas (Duerr and Ahearn, 1996).

Na⁺/H⁺ antiporters, epithelial Na⁺ channels and Na⁺/K⁺/2Cl⁻ cotransporters have been considered as candidates in the uptake of Na⁺ by gills of euryhaline crabs living in low salinities (Lucu and Siebers, 1986; Burnett and Towle, 1990; Lucu, 1993). In the green shore crab *Carcinus maenas* as well as the Chinese crab *Eriocheir sinensis*, electrophysiological evidence has been presented for the participation of amiloride-sensitive Na⁺ channels in this process (Onken and Siebers, 1992; Zeiske *et al.* 1992). However, in perfused gills of the blue crab *Callinectes sapidus*, under conditions closely resembling those found *in vivo*, amiloride blocks transport of Na⁺ against a transepithelial concentration gradient only at inhibitor concentrations far exceeding those expected to block epithelial Na⁺ channels

*e-mail: towle@lfc.edu.

(Burnett and Towle, 1990). In gills of *Carcinus maenas*, amiloride treatment results in an alteration of transepithelial potentials in a manner consistent with the electrogenic properties of an apical Na^+/H^+ antiporter (Siebers *et al.* 1989), although the authors interpret their findings as support for the participation of conductive Na^+ channels in the uptake process. Recently, evidence has been obtained for a possible role of $\text{Na}^+/\text{K}^+/\text{2Cl}^-$ cotransporters in ion uptake across split gill preparations of *Carcinus maenas* (Riestenpatt *et al.* 1996).

To explore more completely the molecular properties of Na^+/H^+ antiporters in gills of euryhaline crabs and to seek information that would permit differentiation between the role of antiporters, cotransporters and channels in the Na^+ uptake process, we set out to identify and sequence antiporter cDNA derived from mRNA of *Carcinus maenas* gill. The first Na^+/H^+ antiporter of animal cells to be sequenced was the Na^+/H^+ exchanger (NHE-1) of human cells (Sardet *et al.* 1989, 1990). Translation of the human cDNA nucleotide sequence to the predicted 815-amino-acid antiporter protein sequence revealed alternating regions of marked hydrophobicity and hydrophilicity characteristic of a membrane protein containing 10 or 12 membrane-spanning domains (Bianchini and Pouyssegur, 1994). The four mammalian isoforms so far described in the literature exhibit similar hydrophobicity patterns, suggesting that their native structures within the plasma membrane are similar. Indeed, when amino acid sequences of the different isoforms are compared and aligned, high degrees of homology are noted, particularly within the putative transmembrane domains.

The highly conserved nature of the vertebrate Na^+/H^+ antiporters analyzed to date suggested to us that the electrogenic and electroneutral Na^+/H^+ antiporters of crustaceans might be amenable to characterization using molecular biological techniques based on the vertebrate sequences, despite the functional distinction in the stoichiometry of exchange in one of the crustacean forms. Our demonstration of hybridization under low-stringency conditions between crab gill RNA and a cDNA probe representing the human antiporter isoform NHE-1 suggested that an antiporter related to the vertebrate isoforms is indeed expressed in crustacean cells (Towle *et al.* 1992).

Materials and methods

Animals

Specimens of the green shore crab (*Carcinus maenas* L.) were collected from intertidal regions near Mount Desert Island Biological Laboratory in Salsbury Cove, Maine, or were obtained from the Marine Resources Department of the Marine Biological Laboratory, Woods Hole, Massachusetts. At Mount Desert Island, the animals were maintained in flowing natural sea water (32–33‰, 10–15 °C) and fed mussel pieces twice weekly. At Lake Forest, crabs were kept at 15 °C in recirculating, biologically filtered Instant Ocean sea water (40‰) and were fed cleaned squid twice weekly.

African clawed frogs (*Xenopus laevis* Daudin) obtained from NASCO were maintained at 18 °C in a 12h:12h

light:dark cycle. They were kept in pairs in 10-l plastic tanks containing 5 cm of dechlorinated tap water. Frogs were fed 'frog brittle' twice a week, followed by a change of water 1 h after feeding.

RNA and cDNA preparation from *Carcinus maenas* gill

The posterior three gills, containing substantial numbers of columnar ionocytes (Towle and Kays, 1986; Goodman and Cavey, 1990), were removed from crabs following ice anesthesia. Total RNA was prepared by homogenization in guanidinium isothiocyanate (Chomczynski and Sacchi, 1987) using materials supplied by Promega Corporation. Messenger RNA was prepared for some experiments by direct extraction and binding to oligo-dT-cellulose (FastTrack, Invitrogen). The integrity of RNA preparations was confirmed using formaldehyde-containing agarose gels (Ausubel *et al.* 1992). It should be noted that ribosomal RNA from crab tissues produces three electrophoretic bands under these conditions, an observation noted previously in other laboratories (C. Paulson, personal communication).

Single-stranded cDNA was reverse-transcribed from total RNA using AMV reverse transcriptase (Stratagene) with oligo-dT as the primer or from mRNA using SuperScript II RNAase H⁻ reverse transcriptase (Gibco-BRL) and oligo-dT or antiporter-specific primers.

Amplification of central fragment of crab antiporter cDNA

Degenerate primers based on conserved sequences in Na^+/H^+ antiporters from human (Sardet *et al.* 1989), pig (Reilly *et al.* 1991) and trout (Borgese *et al.* 1992) were initially designed to target an approximately 700-base-pair (bp) cDNA fragment encoding six putative transmembrane segments of the antiporter protein. Sequences of these primers (3F and 4R) and all other oligonucleotides designed for this study were obtained with the assistance of OLIGO 4.1 software and are given in Table 1. A third degenerate primer, 5A, was designed to amplify independently a slightly larger (approximately 800 bp) but completely overlapping fragment of crab gill cDNA when used with primer 4R.

The polymerase chain reaction (PCR) was performed by the hot-start method using Taq polymerase (Promega or Boehringer-Mannheim) in Inotech or MJ Research thermal cyclers. Initial amplification of a 700 bp antiporter sequence from cDNA derived from total RNA of *C. maenas* gill was accomplished using primers 3F and 4R with five cycles of 94 °C (90 s), 40 °C (30 s) and 72 °C (120 s), followed by 45 cycles of 94 °C (90 s), 45 °C (30 s) and 72 °C (120 s) and a final incubation at 72 °C for 5 min.

PCR products were analyzed by electrophoresis in 0.8 % to 1 % agarose gels using 1× Tris–borate–EDTA or 1× Tris–acetic acid–EDTA buffer (Ausubel *et al.* 1992). Nucleic acid bands were visualized by staining the gels with ethidium bromide (1 mg l⁻¹) and photographing over an ultraviolet lightbox.

Ligation and cloning

Individual PCR bands were cut from the agarose and the

Table 1. Sequences of oligonucleotide primers employed to identify and amplify antiporter cDNA from *Carcinus maenas*

Primer name	Nucleotide position	Nucleotide sequence of primer and corresponding amino acid sequence
Degenerate sense primers		
3F	1178–1197	5'-AA(C/T) GA(C/T) G(C/G)I GTI ACI GTI GT-3' N D G V T V V
5A	1091–1122	5'-GTG GAC CC(C/G/T) GTG GC(C/G/T) GT(G/T)- V D P V A V- CT(C/G/T) GC(C/G/T) GT(C/G/T) TT(C/T) GA-3' L A V F E
Degenerate anti-sense primer		
4R	1871–1890	5'-GG IC(G/T) IAT IGT IAT ICC (C/T)TG-3' P K I T I G Q
Non-degenerate sense primers		
9F	1768–1791	5'-G GTG GCC TTT GCT CTC GTC ATC AC-3' V A F A L V I T
20F	1128–1151	5'-TG CAA GTG GAG GAG GTG CTG TTT A-3' M Q V E E V L F
F160	160–179	5'-GG GAA GGC AGT AGC AGT TTA T-3' (non-coding region)
Non-degenerate anti-sense primers		
R1	1202–1225	5'-ACT GAA GCC CTC GAA CAG GTG ATA-3' S F G E F L H Y
R2	1249–1269	5'-CC GCT AGC TAT GTC CAC CGC C-3' G S A I D V A
21R	1793–1816	5'-GAG TGG GAT GTG GAT TGG GTT GAT-3' L P I H I P N I
R2162	2165–2184	5'-TAC AAC GCT TCT ACC AAC AT-3' Y N A S T N I

Nucleotide positions and amino acid equivalents are given in relation to the crab antiporter sequence reported in Fig. 3.

For the degenerate primers, the *Carcinus* amino acid sequence does not always coincide with the primer nucleotide sequence.

DNA purified by adsorption onto resin (Wizard PCR Preps, Promega). The purified PCR products were ligated into pCRTMII (Invitrogen) or pGEM-T (Promega) plasmid vectors, which were then used to transform competent XL1-Blue *Escherichia coli*. Following overnight incubation, recombinant plasmids were isolated by alkaline detergent lysis (Wizard Minipreps, Promega) and analyzed by restriction digestion and agarose gel electrophoresis for the presence of an appropriately sized insert. Some inserts were subcloned into M13 phage vectors (M13mp18RF and M13mp19RF; GibcoBRL) prior to sequencing.

Amplification and sequencing of the 5' region of crab antiporter cDNA

Non-degenerate, *Carcinus*-specific oligonucleotide primers based on the sequence initially determined for the central

800 bp fragment of the *C. maenas* antiporter were designed with the assistance of OLIGO software (Table 1). To obtain cDNA for amplification of the 5' region of the antiporter, messenger RNA purified from posterior gill was reverse-transcribed using primer R2 and SuperScript II reverse transcriptase. The resulting cDNA was anchor-ligated using the 5'-Amplifinder kit (Clontech). PCR amplification was performed on the resulting template using the Clontech anchor primer and the *Carcinus*-specific primer R1, cycling 35 times at 94 °C (45 s), 60 °C (45 s) and 72 °C (120 s). A single 1.37 kilobase (kb) product was recovered from the electrophoresis gel and ligated into pGEM-T (Promega) plasmid vector for transformation into XL1-Blue *E. coli*. Three independent clones containing an insert of the appropriate size were sequenced on both strands following controlled S1 nuclease deletion (Erase-A-Base, Promega) and subcloning.

Amplification and sequencing of the 3' region of crab antiporter cDNA

Messenger RNA from posterior gill of *C. maenas* was reverse-transcribed using SuperScript II reverse transcriptase and the 3' adapter primer provided with the 3' Rapid Amplification of cDNA Ends (RACE) kit (Gibco-BRL). PCR amplification of the 3' region of the antiporter was achieved using *Carcinus*-specific primer 9F (Table 1) and the Gibco-BRL universal amplification primer, cycling 35 times at 95 °C (60 s), 60 °C (35 s) and 72 °C (135 s). An 800 bp product was ligated into the pGEM-T vector for transformation of XL1-Blue *E. coli*. Four positive clones were sequenced in both directions following S1 nuclease deletion and subcloning into M13 bacteriophage.

Sequencing

Double-stranded plasmids or single-stranded M13 phage containing inserts were sequenced *via* dideoxynucleotide procedures using Sequenase 2.0 polymerase (Amersham Life Science), modified to reduce premature chain terminations (Sanger *et al.* 1977; Kho and Zarbl, 1992), or Cyclist Exo⁻ Pfu polymerase (Stratagene). Sequencing products labeled with ³⁵S[ATP] were analyzed by electrophoresis on denaturing 7 mol l⁻¹ urea–5 % polyacrylamide gels at 55 °C, followed by exposure of the dried gel to X-ray film.

Following completion of the sequencing by conventional means, a nearly complete antiporter nucleotide sequence was amplified from gill cDNA using non-degenerate primers *F160* and *R2162* (Table 1) and 30 cycles of 92 °C (1 min), 40 °C (1 min) and 72 °C (2 min) followed by extension at 72 °C (5 min). The predicted 2025-nucleotide product was purified by agarose electrophoresis, extracted from the gel and partially sequenced (Sequenase PCR product sequencing kit). In addition, the complete 689 bp region of the antiporter defined by primers *20F* and *21R* was directly re-sequenced using as template the PCR product amplified from gill cDNA, revealing three scattered bases which were not detected in the original plasmid sequencing effort.

Sequence analysis

Individual nucleotide sequences were connected and then analyzed for open reading frames using DNASIS software (Hitachi). Related sequences were revealed by searching the GenBank database using the BLAST algorithm (Altschul *et al.* 1990). Predicted amino acid sequences were aligned with other antiporter sequences and a relationship diagram generated using GCG PILEUP and DISTANCES programs (Program Manual for the Wisconsin Package Version 8, 1994, Genetics Computer Group, Madison, WI, USA). Hydrophathy analysis (Kyte and Doolittle, 1982) was performed with PROFILEGRAPH software (Hofmann and Stoffel, 1992) and transmembrane α -helices were predicted using MEMSAT software (Jones *et al.* 1994).

Functional expression in Xenopus laevis oocytes

The complete *C. maenas* antiporter sequence was assembled

via PCR (Higuchi, 1990) and inserted into the multiple cloning site of plasmid pcDNA3 (Invitrogen) downstream from the T7 promoter. The recombinant plasmid was cut at an *Apa*I restriction site downstream from the antiporter insert and was then employed as template in the production of antiporter cRNA using Promega's T7 RiboMAX kit. Following poly-A tailing with poly-A polymerase (Gibco-BRL), the RNA product was precipitated with isopropanol at –20 °C overnight, centrifuged at 10000g for 1 h at 4 °C, washed with ice-cold 75 % ethanol, dried in air, and then resuspended in RNAase-free water at a final concentration of 1 μ g μ l⁻¹ for oocyte injection.

Oocytes at Dumont stages V and VI were surgically removed from ice-anesthetized *Xenopus laevis* and were separated from the ovarian lobes using fine forceps. Following collagenase treatment for 1 h, defolliculated oocytes were allowed to recover in Barth's medium (Colman, 1984) overnight at 18 °C. Antiporter cRNA (50 ng in 50 nl) or RNAase-free water (50 nl) was injected into individual oocytes using a World Precision Instruments nanoliter injector. The oocytes were then maintained at 18 °C in daily changes of Barth's medium for 96 h.

H⁺ efflux from oocytes was measured by incubating 10 oocytes (uninjected, water-injected or antiporter-cRNA-injected) in 100 μ l of weakly buffered incubation medium [0.5 mmol l⁻¹ Hepes–Tris, pH 7.4, 0.33 mmol l⁻¹ Ca(NO₃)₂, 0.41 mmol l⁻¹ CaCl₂, 0.82 mmol l⁻¹ MgSO₄ containing 104 mmol l⁻¹ NaCl (experimental) or choline chloride (control)] (George *et al.* 1989; Towle *et al.* 1991). A miniature pH electrode (Microelectrodes Inc.) was placed in the buffer, which was then covered with 50 μ l of light mineral oil. Changes in pH of the medium were monitored over approximately 30 min periods.

Semi-quantitative reverse transcription–polymerase chain reaction (RT-PCR) analysis of antiporter mRNA levels

Total RNA preparations from different tissues of *Carcinus maenas* were treated with RNAase-free DNAase (Gibco-BRL) to remove genomic DNA contaminants and were assayed for RNA content by spectrofluorometry in ethidium bromide solutions ($\lambda_{\text{ex}}=546$ nm, $\lambda_{\text{em}}=590$ nm) (Ausubel *et al.* 1992). Starting with 2 μ g of total RNA, poly-A⁺ RNA was reverse-transcribed (SuperScript II reverse transcriptase, Gibco-BRL) using oligo-dT as primer. 5 % of the resulting single-stranded cDNA (1 μ l of the 20 μ l reverse transcription volume) was used as template for amplification of a 689-nucleotide antiporter sequence using *Carcinus*-specific primers *20F* and *21R* (Table 1). These primers were designed to anneal to non-conserved regions of the antiporter cDNA, thus minimizing the likelihood of amplification of other closely related sequences.

Accumulation of the 689 bp PCR product was estimated by replacing 16.7 % of the dTTP in the PCR reaction mixture with biotin–dUTP (Clontech). Following a hot-start addition of Taq polymerase, amplification proceeded for 22, 24 or 26 cycles at 92 °C (35 s), 60 °C (35 s) and 72 °C (35 s), followed by a final extension at 72 °C (120 s). PCR products were separated on a

0.8% agarose electrophoresis gel which was then soaked in two 30 min washes each of denaturing solution (0.5 mol l⁻¹ NaOH/1.5 mol l⁻¹ NaCl) and then neutralizing solution (1 mol l⁻¹ Tris/1.5 mol l⁻¹ NaCl). The PCR products were transferred to a nylon filter membrane (Immobilon S, Millipore) in 20× standard saline citrate (SSC) overnight. After baking the membrane filter at 80 °C for 2 h, biotinylated products on the filter were localized using streptavidin and biotinylated alkaline phosphatase (New England Biolabs Phototope System).

Semi-quantitative RT-PCR estimation of actin mRNA in crab tissues

To control for possible hydrolysis of antiporter mRNAs, particularly in the RNAase-rich hepatopancreas, actin mRNA levels were estimated in each total RNA extract used for antiporter mRNA quantitation. Published actin cDNA sequences from crayfish *Procambarus clarkii* (Kang and Naya, 1993), brine shrimp *Artemia franciscana* (Macias and Sastre, 1990) and fruit fly *Drosophila melanogaster* (GenBank Accession number K00670) were aligned to reveal conserved sequences. Degenerate oligonucleotide primers were then designed to anneal with two such regions. The forward primer had the following composition: 5'-GTC GG(C/T) GA(C/T) GA(G/A) GC(A/T) CA(G/A) AGC AA-3'; the reverse primer was: 5'-GG(G/A) CA(G/A) CGG AA(A/T) CG(C/T) TCA TT-3'. Following DNAase treatment and reverse transcription of 2 µg of total RNA, 5% of the resulting cDNA was employed as template for PCR, which was carried out in the presence of biotin-dUTP at 92 °C (1 min), 45 °C (1 min) and 72 °C (2 min) for 20–24 cycles followed by 72 °C for 5 min. Amplification products were separated by electrophoresis and transferred to nylon membranes. The expected 613 bp actin cDNA amplification fragment was then visualized as described above. Negative controls in which the reverse transcriptase was omitted were analyzed in parallel. Omitting the DNAase treatment resulted in the appearance of amplification products in these negative controls, apparently the result of amplification of genomic actin DNA. It should be noted that antiporter-specific primers *20F* and *21R* produced true negative controls with or without DNAase treatment of RNA samples.

Results

Oligonucleotide primers *3F* and *4R*, based on conserved regions of several vertebrate Na⁺/H⁺ antiporter sequences,

Fig. 2. Strategy for amplification and sequencing of complete *Carcinus maenas* Na⁺/H⁺ antiporter cDNA. Degenerate primer pairs *3F+4R* and *5A+4R* supported amplification of 713 bp and 800 bp fragments, respectively, as illustrated in Fig. 1. *Carcinus*-specific primers *R1* and *9F* were then used with RACE primers to amplify the 5' and 3' ends of the antiporter cDNA. Controlled deletion and subcloning were followed by bidirectional sequencing, yielding a 2595-nucleotide sequence.

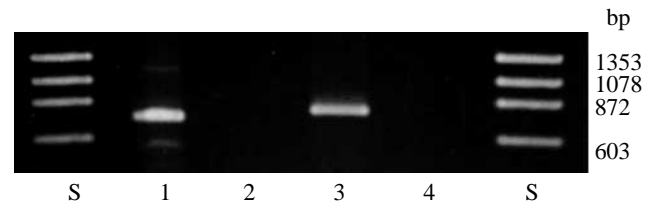


Fig. 1. PCR-based amplification of an approximately 700 bp product from *Carcinus maenas* gill cDNA using degenerate Na⁺/H⁺-antiporter primers *3F* and *4R* (lane 1) and an approximately 800 bp product using degenerate antiporter primers *5A* and *4R* (lane 3). Lanes 2 and 4 contained samples treated identically to those in lanes 1 and 3, respectively, except omitting reverse transcriptase. Sizes in base pairs (bp) are given for DNA molecular mass standards, ϕ X174 DNA digested with *Hae*III endonuclease (lanes S).

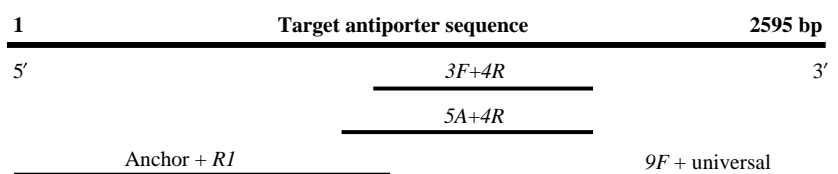
were successful in supporting amplification of a discrete product using *C. maenas* gill cDNA as the template (Fig. 1). The size of the PCR product (approximately 700 bp) matched the expected size based on vertebrate antiporter sequence comparisons. More importantly, the nucleotide sequence of the *3F–4R* fragment exhibited 58–62% identity with the homologous region of the mammalian antiporters.

An independent amplification of *C. maenas* antiporter cDNA was accomplished using primers *5A* and *4R*, producing an 800 bp product (Fig. 1) whose sequence completely overlapped the *3F–4R* fragment. We thus became convinced that we had identified a crustacean cDNA sequence related to the published vertebrate Na⁺/H⁺ antiporter sequences, and proceeded to amplify and sequence the remainder of the *C. maenas* cDNA sequence using RACE techniques.

Employing controlled deletion methods and subcloning into M13 bacteriophage, overlapping segments of each cDNA strand were sequenced in both directions in at least three separate experiments for each segment (Fig. 2). A particular nucleotide sequence was accepted when data from at least two independent clones agreed.

The completed *C. maenas* Na⁺/H⁺ antiporter sequence consists of a 2595-nucleotide cDNA with a 2019-nucleotide open reading frame (Fig. 3). The probable start codon (ATG) lies 455 nucleotides from the 5' end of the cDNA. An in-frame stop codon is situated nine bases upstream from the probable 5' start site, and several additional stop codons precede it. Two overlapping poly-A signals (AATAAA) lie 75 bases downstream from the initial 3' stop codon, followed in 14 bases by the poly-A tail itself.

Non-degenerate primers *F160* and *R2162*, based on the



1	G AGT CAG CTG GTG GAC GTC AGG GAG GGA AGA CCA TGG CCG CTT CTT TCC TCG CCT TGC TCA CTC CAT AAC CCT TTC TCG TCT TTG GCA	88
89	TCA CCT CAC AAC TAG TAC CGT CCC TCA CGT CAT CTC CCA GTA CAA TAT CCA GGA CTC TAA CAC AGC GAG AGG GAA GGC AGT AGC AGT TTA	178
179	TAA GTA CTA GTG AAA ACA GAA AAG TTG TCA CCT CTC TTG TGT GTC GAG TGA AAC CCG CCC GTG AGT GCA TTG CTA GCT GGA AAA GAG TTA	268
269	TCC TAG TAC GTA CCT CAA ACT TAT AAT ACA CTC TAA AAT AAC CAC GTA AAT CTC TTC ATA TAC ACT TAA ACC CTT TGT CCG TGA GTG TAG	358
359	TAG TCA AAA CTA GTC ATA CGT TAC TCC GGT GCT TGG AAA CGG ACG GAT TTT CTA AAT AAA CCG CAA CGG TTC TTA TAC AAA AAC CAA TAA	448
449	ATC ATC ATG AAG AAC AGG GTA ATA TTA ATG GTG TGT GTG GCG TGG TGT GTG TTG GGT CTG GCT GCT GCT AAC ACC TCG GCT AAG CAA CAC	538
1	M K N R V I L M V C V A W C V L G L A A A N T S A K Q H	28
539	CAC ACA GCC ACC AAC ACC ACC ACC GCT GAT AAT GAA ACA CTG CAA CGT GTT CGA ATA GAC GGG AGT GAG GCA CAT AAT GAA GCA GAA	628
29	H T A T N T T T T A D N E T L Q R V R I D G S E A H N E A E	58
629	GGT GAA CAT CGG TTA GAG AGA TAC CCT GTG GTG GTG TTG GAC TTT GAG AGG GTA CAG ACG CCC TTC ATC GGT CTG TGG ATC TTC CTG GCG	718
59	G E H R L E R Y P V V V L D F E R V Q T P F I G L W I F L A	88
719	TGT TTG GGC AAG ATT GGC TTC CAC ATG ACT CCG AAG ATC TCT CAC GTC TTC CCG GAG TCG TGC ATG TTG ATC GTC CTA GGA GTC CTG ATT	808
89	C L G K I G F H M T P K I S H V F P E S C M L I V L G V L I	118
809	GGC TTG CTG CTC ATC TAC ACC CAG GCA GCC ACG GTA TCT CCC CTC ACA GCT GAC GTG TTC TTC CTC TAC CTC CTC CCC CTC ATC ATC CTA	898
119	G L L L I Y T Q A A T V S P L T A D V F L Y L P P I I L	148
899	GAC GCC GTT TAC TTC ATG CCA AAC CGA CTC TTC TTT GAT AAT CTC TTC ACC ATC TTG GTT TTC GCG GTG ATT GGC ACG ATC TGG AAC GCG	988
149	D A V Y F M P N R L F F D N L F T I L V F A V I G T I W N A	178
989	CTG ACT ATT GGA ATC ACT ATG TAC GCT ATT AGC CTG ACG GGG CTG TTT GGG CTA GAC ATT CCG ATG CTC CAC ATG TTC CTG TTC TCG TCT	1078
179	L T I G I T M Y A I S L T G L F G L D I P M L H M F L F S S	208
1079	CTC ATC TCC GCC GTG GAC CCC GTG GCT GTG CTG GCC GTG TTC GAG GAG ATG CAA GTG GAG GAG GTG CTG TTT ATC TTA VTG TTC GGG GAG	1168
209	L I S C V D P V A V L A V F E E M Q V E E V L F I L V P F G E	238
1169	TCA CTT CTC AAT GAT GGT GTG ACG GTG GTA CTG TAT CAC CTG TTC GAG GGC TTC AGT GAG TTA GGG GAA GCA AAC ATC ATG GCG GTG GAC	1258
239	S L L N D G V T V V L Y H L F E G F S E L G E A N I M A V D	268
1259	ATA GCT AGC GGC GTG GCA TCC TTC CTC CTG GTG GCA CTG GGC GGC ACT GCT ATT GGC ATC ATC TGG GGC TTC CTT ACT GCC TTC GTC ACC	1348
269	I A S G V A S F L L V A L G G T A I G I I W G F L T A F V T	298
1349	AGG TTA ACG AGT GGA GTA CGA GTA ATC GAG CCT GTG TTT GTG TTC GTG ATG GCT TAC CTG GCT TAC CTC AAC GCT GAG ATC TTC CAC CTG	1438
299	R L T S G V R V I E P V F V F V M A Y L A Y L N A E I F H L	328
1439	TCG GGC ATC TTG TCC ATC ACC TTC TGC GGC ATC ACT ATG AAG AAC TAC GTG GAA CAG AAC ATC TCC GCC AAG TCC CAC ACG ACC ATC AAA	1528
329	S G I T S I T Q A A C K N I S A K I S A K I T I K	358
1529	TAC GCC ATG AAG ATG TTA GCC TCG TCT TCG GAG ACC ATC ATC TTC ATG TTC CTG GGA GTG TCC ACC ATT CAG AGT GAT CAC CAG TGG AAC	1618
359	Y A M K M L A S S S E T I I F M F L G V S T I Q S D H Q W N	388
1619	ACG TGG TTT GTC ATC CTC ACC ATC CTC TTC TGC TCC ATC TAC CGT ATT CTA GGA GTG CTC ATC TTC AGC GCG GTA TGT AAC AGA TTC CGC	1708
389	T W F V I L T I L F C S I Y R I L G V L I F S A V C N R F R	418
1709	GTC AAG AAG ATC GGT TTT GTG GAC AAG TTT GTG ATG AGT TAC GGA GGG TTG CGA GGA GCG GTG GCC TTT GCT CTC GTC ATC ACC ATC AAC	1798
419	V K K I G F V D K F V M S Y G G L R G A V A F A L V A I T I N	448
1799	CCA ATC CAC ATC CCA CTC CAG CCC ATG TTC CTT ACT GCT ACT ATT GCC ATG GTC TAC TTC ACC GTG TTC GTA CAG GGC ATC ACA ATT AAG	1888
449	P I H I P L Q P M F L T A T I A M V Y F T V F V Q G I T I K	478
1889	CCT CTC GTT CAG CTT TTG GGA GTG AAG AAA TCT GAG AAG AGG AGT CTA ACG ATG AAC GAG AGA TTG CAC GAA AGG GTG ATG GAT TAC GTT	1978
479	P L V Q L L G V K K S E K R S L T M N E R L H E R V M D Y V	508
1979	ATG TCT GGC GTG GAG GAA ATG ATT GGC AAG CAG GGG AAC CTT CAT ATT AGA AGC AAG TTC AAG CGG TTC AAC AAC AAG TAC CTC ACG CCC	2068
509	M S G V E E M I G K Q G N L H I R S K F K R F N N K Y L T P	538
2069	TTC CTG GTA CGG GAG AAG AAC GTG ATT GAA CCC AAA CTC ATC GAG ACC TAC AGT AAC ATC AAG AAG CAC GAG GCC ATG CAA CAG ATG CAC	2158
539	F L V R E K N V I E P L I E T Y S N I K K H E A M Q Q M H	568
2159	AAC AGT TAC AAC GCT TCT ACC AAC ATT GAA TCC TTC TCT AAC CTT ATT CGT AAT GAT GCC ACT CAT CCA CAT GTA CAA ATG AAC AAC CAA	2248
569	N S Y N A S T N I E S F S N L I R N D A T H P H V Q M N N Q	598
2249	GGA GAA TGG AAT CTG GAT GTG GCT GAG CTG GAA TAC AAC CCA ACA CTA AGA GAC CTC AAT GAT GCT AAG TTC CAC CAC CTC CTC TCC AAT	2338
599	G E W N L D V A E L E Y N P T L R D L N D A K F H H L L S N	628
2339	GAT TAC AAG CCA GTC AAA AAG AAT CGC GCC TCC ACC TAC AAG AGA CAC GCG GTC AAA GAT GAT GAC ATG CAG ACA CAA TCG GAT ATC GGC	2428
629	D Y K P V K K N R A S T Y K R H A V K D D M Q T Q S D I G	658
2429	CAC CAC AAC ATG TAC CTC CAC ACA CAC ACA CAC ACA CAA TTA TTA TGA TGA AGG AGA AAT GTT ATA GAA ATA TTG TAC TGT AAA ATA GGA	2518
659	H H N M Y L H T H T H T Q L L	673
2519	CTT AGT TTT GTC TCC TGT TGT GTC TTG TAA ATA AAT AAA TTA AGA GAA AGA TAA AAA AAA AAA AAA AAA AAA AA	2595

Fig. 3. Nucleotide sequence and predicted amino acid sequence of *Carcinus maenas* Na⁺/H⁺ antiporter. Boxes (red) in the 5'-region indicate multiple in-frame stop codons upstream from the putative translation initiation site, which is followed by a 2019-nucleotide open reading frame. The rectangle (yellow) at nucleotide position 2548 indicates overlapping polyadenylation signals (AATAAA) downstream from repeated termination codons (TGA). Underlines (green) indicate predicted transmembrane domains of the antiporter protein (see Fig. 10) (GenBank Accession number U09274).

sequences of the three overlapping fragments indicated in Fig. 2, successfully amplified a predicted 2025-nucleotide product directly from cDNA of *C. maenas* gill (Fig. 4),

indicating that the sequence presented in Fig. 3 is a faithful representation of the native antiporter. Partial sequencing of this product confirmed our conclusion that we have indeed

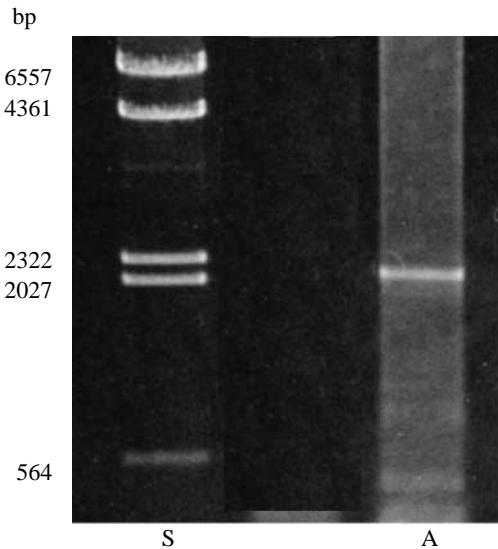


Fig. 4. Amplification of a nearly complete antiporter sequence from *Carcinus maenas* gill cDNA using non-degenerate primers *F160* and *R2162*, based on the sequence reported in Fig. 3. A predicted 2025 bp amplification product resulted (lane A). DNA molecular mass standards (λ DNA digested with *Hind*III endonuclease) are presented in lane S.

identified a complete Na^+/H^+ -antiporter-like sequence from green shore crab gill.

Furthermore, a search of the GenBank database using the BLAST algorithm (Altschul *et al.* 1990) revealed more than 20 high-scoring matches with the putative crab antiporter sequence. These matches were exclusively Na^+/H^+ antiporter sequences from various vertebrate species (Sardet *et al.* 1989; Hildebrandt *et al.* 1991; Reilly *et al.* 1991; Tse *et al.* 1991, 1992; Borgese *et al.* 1992; Orłowski *et al.* 1992; Collins *et al.* 1993; Counillon and Pouysségur, 1993b) plus several related sequences from an invertebrate, the nematode *Caenorhabditis elegans* (Marra *et al.* 1993).

Preliminary evidence for the functionality of the cloned antiporter was offered by injecting into *Xenopus* oocytes cRNA transcribed from the complete antiporter plasmid construct. Water-injected oocytes exhibited Na^+ -dependent H^+ efflux rates similar to those of uninjected oocytes, while oocytes injected with the putative *C. maenas* antiporter cRNA exhibited approximately sevenfold greater H^+ efflux rates (Fig. 5). When Na^+ in the incubation medium was completely replaced with choline, H^+ efflux rates were not statistically different from zero (data not shown), indicating that the observed H^+ efflux resulted from Na^+/H^+ exchange. It should be stated that oocytes expressing the exogenous antiporter were extremely fragile, making it impossible to repeat experiments on the same group of oocytes. Thus, our efforts to determine the kinetic characteristics of the cloned antiporter have so far proved unrewarding.

To examine antiporter mRNA levels in various tissues of the crab, we employed semi-quantitative reverse transcription-polymerase chain reaction (RT-PCR). An estimate of steady-

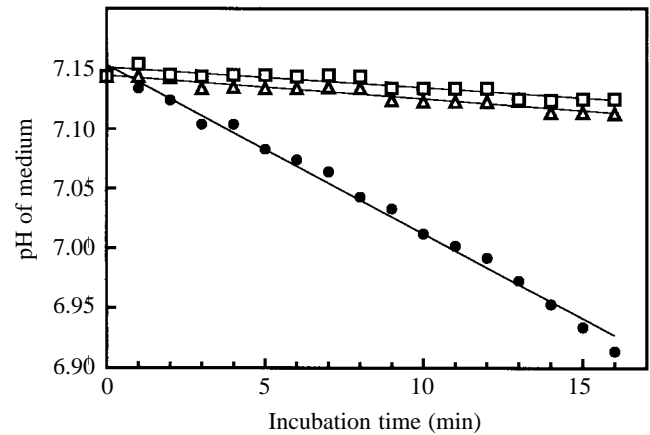


Fig. 5. Na^+ -dependent H^+ efflux from *Xenopus laevis* oocytes which were uninjected (open squares), injected with water (open triangles) or injected with cloned antiporter cRNA from the crab *Carcinus maenas* (filled circles). Ninety-six hours after injection, oocytes were incubated in weakly buffered medium containing Na^+ (104 mmol l^{-1}). Oocytes incubated in nominally Na^+ -free medium (104 mmol l^{-1} choline) exhibited H^+ efflux rates which were not significantly different from zero (data not shown). Representative of three individual experiments.

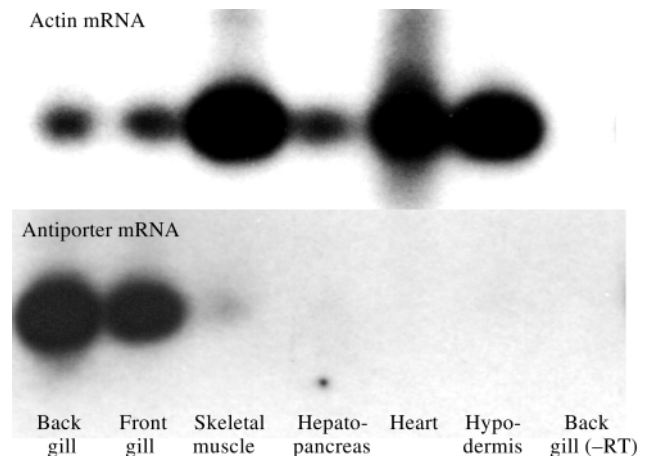


Fig. 6. Estimation of actin mRNA and antiporter mRNA levels in tissues of the green crab *Carcinus maenas*, using semi-quantitative RT-PCR in the presence of biotin-dUTP. Total RNA ($2 \mu\text{g}$) was prepared from each tissue, treated with RNAase-free DNAase and reverse-transcribed using oligo-dT as primer. 5% ($1 \mu\text{l}$ of $20 \mu\text{l}$) of the single-stranded cDNA product was used as template for PCR-catalyzed amplification of actin or antiporter cDNA using degenerate arthropod actin primers or *Carcinus*-specific antiporter primers (*20F* and *21R*) respectively. In separate experiments, we showed that product appearance continued to be linear at 24 cycles for actin cDNA and 26 cycles for antiporter cDNA, the conditions employed in these experiments. RT, reverse transcriptase.

state mRNA levels using RT-PCR depends upon conditions in which template availability is the major factor limiting the formation of amplification product. Conventional ethidium bromide staining requires large amounts of product for

visualization, typically produced under conditions of saturating template and high cycle number. We thus devised a PCR procedure which incorporated biotin-dUTP into the amplification products, formed with low (and limiting) template levels and relatively low cycle numbers (20–26 cycles). To reduce the likelihood of amplifying related antiporter sequences, we used specific (non-degenerate) oligonucleotide primers (20F and 21R, Table 1) based on non-conserved regions of the 2.6 kb *C. maenas* antiporter sequence. Visualization of biotinylated products with streptavidin and biotinylated alkaline phosphatase showed dependence of product formation on both template concentration and cycle number under these conditions. Thus, the method as developed was useful for estimating steady-state levels of antiporter mRNA.

To ascertain whether RNA extracted from certain tissues, particularly the hepatopancreas, might be subjected to hydrolysis by endogenous ribonucleases, we estimated the levels of actin mRNA, the product of a presumed housekeeping gene, in each sample of total RNA. Beginning with equal amounts of total RNA (2 µg) and amplifying a constant proportion (5 %) of the resulting cDNA, we found that actin mRNA levels were high in skeletal muscle, heart and hypodermis, with lower levels in posterior gill, anterior gill and hepatopancreas (Fig. 6). It is apparent that all tissues including hepatopancreas express actin mRNA, albeit to different degrees, indicating that endogenous RNAases are not destroying mRNA in the tissue samples.

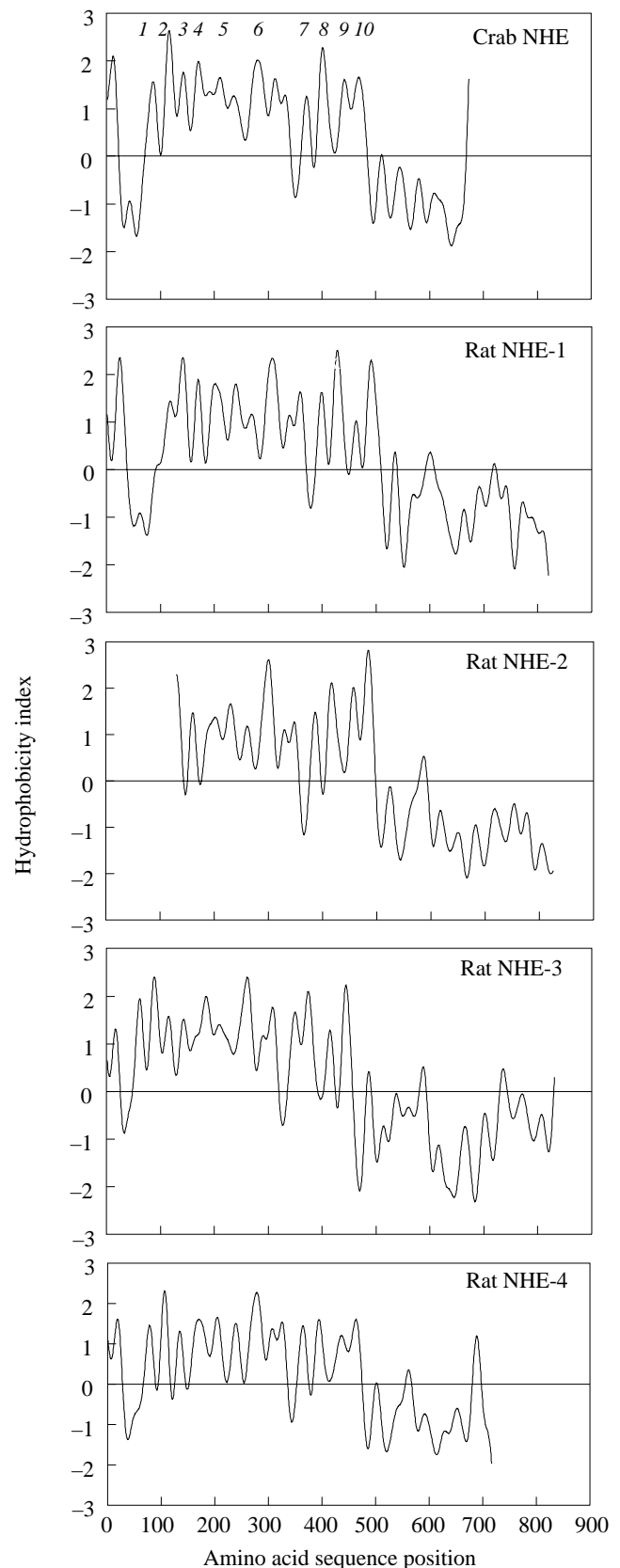
When we applied the semi-quantitative RT-PCR method to estimating antiporter mRNA levels, we found the highest steady-state levels of Na⁺/H⁺ antiporter mRNA in posterior and anterior gill, followed by successively lower levels in skeletal muscle, hepatopancreas, hypodermis and heart (Fig. 6). Although hepatopancreas and gill demonstrate similar levels of actin mRNA, it is clear that the level of antiporter mRNA expression is much higher in gill, with posterior gill possibly exhibiting slightly higher antiporter expression than anterior gill. We conclude that the 2.6 kb antiporter sequence described here is most strongly expressed in gill, a tissue that is involved in multiple functions in crabs, including ion transport, acid–base homeostasis and ammonia excretion (Taylor and Taylor, 1992).

Discussion

Translation of the open reading frame of *C. maenas* antiporter cDNA predicted a 673-amino-acid protein (Fig. 3).

Fig. 7. Hydropathy plots of Na⁺/H⁺ antiporter amino acid sequences from the crab *Carcinus maenas* and examples from the rat of each of four mammalian isoforms (Orlowski *et al.* 1992; Collins *et al.* 1993). Hydropobicity was calculated over a window of 19 amino acid residues using Fourier-averaging to smooth the data (Hofmann and Stoffel, 1992), more clearly revealing putative transmembrane segments. The rat NHE-2 sequence has been shifted to the right by 130 residues to permit easier comparison of hydropathy profiles.

Hydropathy analysis of this amino acid sequence indicated the existence of 12–13 distinct regions of hydrophobicity, some of



which probably represent sections of amino acid sequence which are buried in the lipid bilayer of the plasma membrane (Fig. 7). Comparison of the hydropathy profile of the *C. maenas* antiporter with examples from the rat of the four different mammalian isoforms (NHE-1, NHE-2, NHE-3 and NHE-4) (Orlowski *et al.* 1992; Collins *et al.* 1993) disclosed a substantial similarity in pattern, suggesting a close resemblance of protein tertiary structures within the bilayer membrane.

Multiple alignment of the *C. maenas* antiporter amino acid sequence with examples of the four mammalian antiporter isoforms revealed a number of regions of substantial homology, particularly in some of the putative membrane-spanning regions (Fig. 8). For example, in predicted transmembrane region 5, the *C. maenas* amino acid sequence and the rat isoforms share 72% amino acid identity.

A relationship diagram based on the multiple alignment

suggested that the crab antiporter is not closely related to any specific isoform of vertebrates, although a slight affinity to NHE-3 sequences is noted (Fig. 9). This isoform is thought to be predominantly apical in mammalian epithelia, suggesting that the cloned crab antiporter may also be localized apically. If this is the case, then the crab antiporter is situated optimally to participate in Na⁺ uptake from the external medium across the gill epithelium.

Prediction of probable transmembrane α -helices with MEMSAT software (Jones *et al.* 1994) permitted the generation of a hypothetical two-dimensional arrangement of the *C. maenas* Na⁺/H⁺ antiporter protein in the plasma membrane of the gill epithelial cell (Fig. 10). Defining a minimum transmembrane α -helix of 22 or 23 amino acid residues led to a software-based prediction of 10 transmembrane domains in the crab antiporter protein, while setting the minimum at 19 or 20 amino acid residues predicted



Fig. 8. Alignment of amino acid sequences of crab NHE and mammalian isoforms NHE-1, NHE-2, NHE-3 and NHE-4 (Orlowski *et al.* 1992; Collins *et al.* 1993), based on analysis by GCG PILEUP software. Regions of conserved amino acids are indicated by the color of shading produced by GENEDOC software (Nicholas, 1996), with red indicating functional agreement between all five sequences and green or yellow indicating agreement between four or three sequences, respectively. Numbers underlined refer to predicted transmembrane domains of the antiporter protein (see Fig. 10).

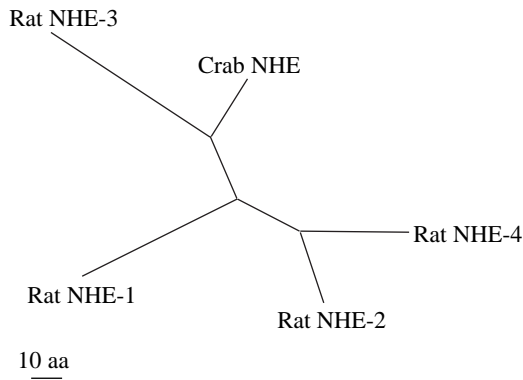


Fig. 9. Relationship diagram of Na⁺/H⁺-antiporter amino acid sequences aligned in Fig. 8 produced by GCG DISTANCES and TREEVIEW (Page, 1996) software. According to this analysis, the crab NHE sequence bears a somewhat closer resemblance to the mammalian NHE-3 isoform than to the other mammalian isoforms. Relationship distances are represented by the length of the connecting lines, the scale representing 10 amino acid substitutions per 100 amino acids.

11 transmembrane domains. Other authors have suggested membrane topologies of 10 (Orlowski *et al.* 1992) or 12

(Bianchini and Pouyssegur, 1994) transmembrane α -helices in the mammalian antiporter proteins. It is likely that the protein contains a signal sequence near the NH₂ terminus, targeting the protein and anchoring it in the plasma membrane.

A striking feature of this model is the abundance of negatively charged amino acid residues in the predicted outwardly facing portion of the antiporter protein (Fig. 10), particularly in an elongated loop which contains no positively charged residues at all. It is possible that the anionic residues in this loop may attract sodium ions in the immediate environment of the antiporter, bringing them to the site of transport within the transmembrane domains of the antiporter protein.

Although software-based analyses of the crab antiporter sequence permit the formation of hypotheses concerning its molecular structure and relatedness to other antiporters, little can be deduced from these studies regarding the role of the antiporter in transbranchial ion movements. Some insight in this regard can be gained, however, from our studies of antiporter mRNA levels in different tissues. Semi-quantitative RT-PCR analysis clearly indicates a high degree of tissue specificity of antiporter mRNA expression. Among the tissues

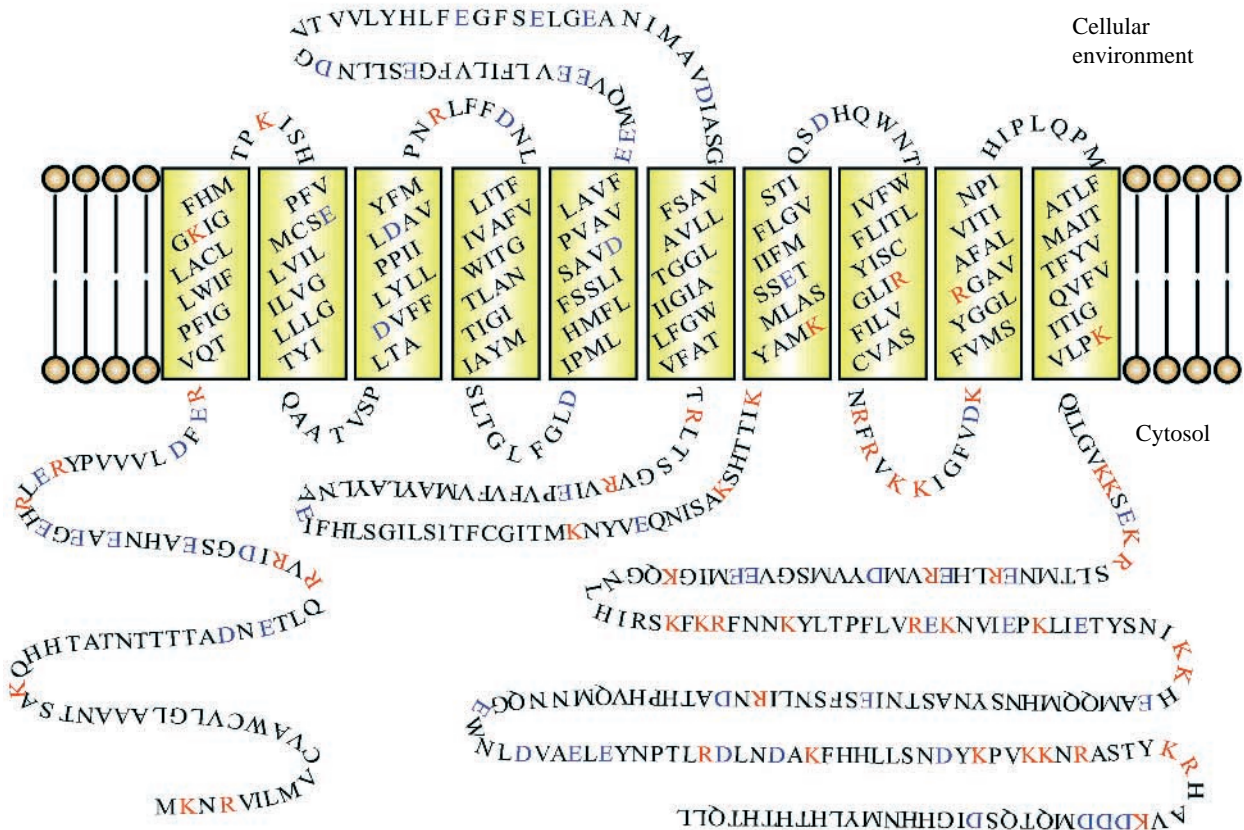


Fig. 10. A hypothetical secondary structure of the crab Na⁺/H⁺-antiporter protein within a lipid bilayer membrane, based on analysis by MEMSAT software (Jones *et al.* 1994) with the minimum transmembrane α -helix length defined as 22 amino acid residues. Ten predicted transmembrane α -helices are separated by extra- and intracellular loops. One elongated extracellular loop is predicted to interact with the cellular environment *via* regions which contain a large excess of negatively charged side chains (blue). The predicted intracellular loop separating transmembrane domains eight and nine contains an abundance of positively charged side chains (red). The extensive intracellular COOH-terminal region probably participates in regulation of the antiporter.

tested, only the posterior and anterior gill appear to accumulate substantial amounts of antiporter mRNA. These are tissues thought to be intimately involved in the ability of euryhaline crabs to take up sodium ions from the aqueous medium (Mantel and Farmer, 1983). Thus, a strong correlation exists between the extent of antiporter mRNA accumulation and the degree of physiological specialization for Na⁺ uptake from the environment.

The low level of antiporter mRNA in crab hepatopancreas may be contrasted with the functional demonstration of electrogenic and electroneutral antiporters in membrane vesicles from lobster hepatopancreas (Ahearn *et al.* 1990; Duerr and Ahearn, 1996). We postulate that the oligonucleotide primers we designed for semi-quantitative RT-PCR are quite gill-specific and, in fact, were selected because they would not anneal to conserved regions of the antiporter sequence. Other antiporter sequences, not detected by gill-specific primers, may predominate in hepatopancreas.

The posterior gills of euryhaline crabs are believed to be particularly specialized for Na⁺ uptake on the basis of high protein-level expression of the Na⁺ pump (Na⁺+K⁺-ATPase) (e.g. Siebers *et al.* 1982; Pequeux *et al.* 1984). In the present study, we detected only a modest difference in antiporter mRNA accumulation between posterior and anterior gills. The high level of antiporter mRNA in all gills may support acid-base regulation and volume regulation in addition to Na⁺ uptake. Studies are under way to ascertain possible changes in antiporter mRNA expression in relation to acclimation salinity. If the antiporter is intimately connected to Na⁺ uptake across the gill, we hypothesize that its mRNA level may increase in low salinity, particularly in posterior gill.

Unfortunately, we remain unable to describe the cloned antiporter sequence in terms of its stoichiometry. Our efforts to study the kinetic properties of the *C. maenas* antiporter using the *Xenopus* oocyte system have so far proved unsuccessful because of the fragility of oocytes expressing the exogenous antiporter. In theory, the kinetic properties of the endogenous *Xenopus* antiporter are sufficiently different from those of the *C. maenas* antiporter to permit differentiation (Shetlar and Towle, 1989; Towle *et al.* 1991). Further work is clearly necessary, possibly using alternative expression systems with antiporter-deficient cell lines.

The present study provides the groundwork for examining the mRNA- and protein-level regulation of Na⁺/H⁺ antiporters in euryhaline crabs acclimating to salinity change, permitting a molecular approach which may not only differentiate between the role of channels, cotransporters and antiporters in the process of Na⁺ uptake across the gill but may also shed light on other physiological processes occurring in the gill. It is clear from this study that *C. maenas* gills vigorously transcribe a gene coding for a Na⁺/H⁺ antiporter. Whether these gills also express a gene coding for an epithelial Na⁺ channel or cotransporter remains to be demonstrated.

The Na⁺/H⁺ antiporter cDNA sequence from the green shore crab *Carcinus maenas* has been accepted by GenBank (Accession number U09274).

This work was supported by the National Science Foundation (DCB-9024293 and IBN-9407261 to D.W.T., plus REU and EPSCoR grants to Mount Desert Island Biological Laboratory), by the American Heart Association (Maine Affiliate) and by the Foster G. McGaw Endowed Chair Fund of Lake Forest College. Sincere thanks are extended to Dr John D. Hempel of the University of Pittsburgh for enabling access to the GCG software package at the Pittsburgh Supercomputing Center (NIH Grant RR06009). We also thank an anonymous referee for suggesting that we re-check the sequence of the central 689-nucleotide segment.

References

- AHEARN, G. A. AND CLAY, L. P. (1989). Kinetic analysis of electrogenic 2 Na⁺-1 H⁺ antiporter in crustacean hepatopancreas. *Am. J. Physiol.* **257**, R484-R493.
- AHEARN, G. A., FRANCO, P. AND CLAY, L. P. (1990). Electrogenic 2 Na⁺/1 H⁺ exchange in crustaceans. *J. Membr. Biol.* **116**, 215-226.
- AHEARN, G. A., ZHUANG, Z., DUERR, J. AND PENNINGTON, V. (1994). Role of the invertebrate electrogenic 2Na⁺/1H⁺ antiporter in monovalent and divalent cation transport. *J. exp. Biol.* **196**, 319-335.
- ALTSCHUL, S. F., GISH, W., MILLER, W., MYERS, E. W. AND LIPMAN, D. J. (1990). Basic local alignment search tool. *J. molec. Biol.* **215**, 403-410.
- AUSUBEL, F. M., BRENT, R., KINGSTON, R. E., MOORE, D. D., SEIDMAN, J. G., SMITH, J. A. AND STRUHL, K. (1992). *Short Protocols in Molecular Biology*, 2nd edn. New York: John Wiley and Sons.
- BIANCHINI, L. AND POUYSSÉGUR, J. (1994). Molecular structure and regulation of vertebrate Na⁺/H⁺ exchangers. *J. exp. Biol.* **196**, 337-345.
- BORGESE, F., SARDET, C., CAPPADORO, M., POUYSSÉGUR, J. AND MOTAIS, R. (1992). Cloning and expression of a cyclic AMP-activated Na⁺/H⁺ exchanger: Evidence that the cytoplasmic domain mediates hormonal regulation. *Proc. natn. Acad. Sci. U.S.A.* **89**, 6765-6769.
- BURNETT, L. E. AND TOWLE, D. W. (1990). Sodium ion uptake by perfused gills of the blue crab *Callinectes sapidus*: effects of ouabain and amiloride. *J. exp. Biol.* **149**, 293-305.
- CHOMCZYNSKI, P. AND SACCHI, N. (1987). Single-step method of RNA isolation by acid guanidinium thiocyanate-phenol-chloroform extraction. *Analyt. Biochem.* **162**, 156-159.
- COLLINS, J. F., HONDA, T., KNOBEL, S., BULLUS, N. M., CONARY, J., DUBOIS, R. AND GHISHAN, F. K. (1993). Molecular cloning, sequencing, tissue distribution and functional expression of a Na⁺/H⁺ exchanger (NHE-2). *Proc. natn. Acad. Sci. U.S.A.* **90**, 3938-3942.
- COLMAN, A. (1984). Translation of eukaryotic messenger RNA in *Xenopus* oocytes. In *Transcription and Translation: A Practical Approach* (ed. B. D. Hames and S. J. Higgins), pp. 271-302. Oxford: IRL Press Ltd.
- COUNILLON, L. AND POUYSSÉGUR, J. (1993a). Molecular biology and hormonal regulation of vertebrate Na⁺/H⁺ exchanger isoforms. In *Molecular Biology and Function of Carrier Proteins* (ed. L. Reuss, J. M. Russell Jr and M. L. Jennings), pp. 169-186. New York: Rockefeller University Press.
- COUNILLON, L. AND POUYSSÉGUR, J. (1993b). Nucleotide sequence of the Chinese hamster Na⁺/H⁺ exchanger NHE1. *Biochim. biophys. Acta* **1172**, 343-345.
- DUERR, J. M. AND AHEARN, G. A. (1996). Characterization of a

- basolateral electroneutral Na^+/H^+ antiporter in Atlantic lobster (*Homarus americanus*) hepatopancreatic epithelial vesicles. *J. exp. Biol.* **199**, 643–651.
- GEORGE, A. L., JR, STAUB, O., GEERING, K., ROSSIER, B. C., KLEYMAN, T. R. AND KRAEHNBUHL, J.-P. (1989). Functional expression of the amiloride-sensitive sodium channel in *Xenopus* oocytes. *Proc. natn. Acad. Sci. U.S.A.* **86**, 7295–7298.
- GOODMAN, S. H. AND CAVEY, M. J. (1990). Organization of a phyllobranchiate gill from the green shore crab *Carcinus maenas* (Crustacea, Decapoda). *Cell Tissue Res.* **260**, 495–505.
- HIGUCHI, R. (1990). Recombinant PCR. In *PCR Protocols: A Guide to Methods and Applications* (ed. M. A. Innis), pp. 177–183. San Diego: Academic Press.
- HILDEBRANDT, F., PIZZONIA, J. H., REILLY, R. F., REBOUÇAS, N. A., SARDET, C., POUYSSÉGUR, J., SLAYMAN, C. W., ARONSON, P. S. AND IGARASHI, P. (1991). Cloning, sequence and tissue distribution of a rabbit renal Na^+/H^+ exchanger transcript. *Biochim. biophys. Acta* **1129**, 105–108.
- HOFMANN, K. AND STOFFEL, W. (1992). PROFILEGRAPH: an interactive graphical tool for protein sequence analysis. *CABIOS* **8**, 331–337.
- JONES, D. T., TAYLOR, W. R. AND THORNTON, J. M. (1994). A model recognition approach to the prediction of all-helical membrane protein structure and topology. *Biochemistry* **33**, 3038–3049.
- KANG, W. AND NAYA, Y. (1993). Sequence of the cDNA encoding an actin homolog in the crayfish *Procambarus clarkii*. *Gene* **133**, 303–304.
- KHO, C.-J. AND ZARBL, H. (1992). A rapid and efficient protocol for sequencing plasmid DNA. *BioTechniques* **12**, 228–230.
- KYTE, J. AND DOOLITTLE, R. F. (1982). A simple method for displaying hydrophobic character of a protein. *J. molec. Biol.* **157**, 105–132.
- LUCU, C. (1993). Ion transport in gill epithelium of aquatic Crustacea. *J. exp. Zool.* **265**, 378–386.
- LUCU, C. AND SIEBERS, D. (1986). Amiloride-sensitive sodium flux and potentials in perfused *Carcinus* gill preparations. *J. exp. Biol.* **122**, 25–35.
- MACIAS, M. T. AND SASTRE, L. (1990). Molecular cloning and expression of four actin isoforms during *Artemia* development. *Nucleic Acids Res.* **18**, 5219–5225.
- MANTEL, L. H. AND FARMER, L. L. (1983). Osmotic and ionic regulation. In *The Biology of Crustacea*, vol. 5, *Internal Anatomy and Physiological Regulation* (ed. L. H. Mantel), pp. 53–161. New York: Academic Press.
- MARRA, M. A., PRASAD, S. S. AND BAILLIE, D. L. (1993). Molecular analysis of two genes between let-653 and let-56 in the unc-22IV region of *Caenorhabditis elegans*. *Molec. gen. Genet.* **236**, 289–298.
- MURER, H., HOPFER, U. AND KINNE, R. (1976). Sodium/proton antiport in brush-border-membrane vesicles isolated from rat small intestine and kidney. *Biochem. J.* **154**, 597–604.
- NICHOLAS, K. (1996). GeneDoc: Multiple sequence alignment editor and shading utility. *Version 1.0.013* (<http://www.cris.com/~ketchup/genedoc.shtml>).
- ONKEN, H. AND SIEBERS, D. (1992). Voltage-clamp measurements on single split lamellae of posterior gills of the shore crab *Carcinus maenas*. *Mar. Biol.* **114**, 385–390.
- ORLOWSKI, J., KANDASAMY, R. A. AND SHULL, G. E. (1992). Molecular cloning of putative members of the Na/H exchanger gene family. cDNA cloning, deduced amino acid sequence and mRNA tissue expression of the rat Na/H exchanger NHE-1 and two structurally related proteins. *J. biol. Chem.* **267**, 9331–9339.
- PAGE, R. D. M. (1996). TREEVIEW: Tree drawing software for Apple Macintosh and Microsoft Windows. *Version 1.2a* (<http://taxonomy.zoology.gla.ac.uk/rod/treeview.html>).
- PEQUEUX, A., MARCHAL, A., WANSON, S. AND GILLES, R. (1984). Kinetic characteristics and specific activity of gill (Na^+/K^+)ATPase in the euryhaline Chinese crab, *Eriocheir sinensis*, during salinity acclimation. *Mar. biol. Lett.* **5**, 35–45.
- REILLY, R. F., HILDEBRANDT, F., BIEMESDERFER, D., SARDET, C., POUYSSÉGUR, J., ARONSON, P. S., SLAYMAN, C. W. AND IGARASHI, P. (1991). cDNA cloning and immunolocalization of a Na^+/H^+ exchanger in LLC-PK₁ renal epithelial cells. *Am. J. Physiol.* **261**, F1088–F1094.
- RIESTENPATT, S., ONKEN, H. AND SIEBERS, D. (1996). Active absorption of Na^+ and Cl^- across the gill epithelium of the shore crab *Carcinus maenas*: voltage-clamp and ion-flux studies. *J. exp. Biol.* **199**, 1545–1554.
- SANGER, F., NICKLEN, S. AND COULSON, A. R. (1977). DNA sequencing with chain terminating inhibitors. *Proc. natn. Acad. Sci. U.S.A.* **74**, 5463–5467.
- SARDET, C., COUNILLON, L., FRANCHI, A. AND POUYSSÉGUR, J. (1990). Growth factors induce phosphorylation of the Na^+/H^+ antiporter, a glycoprotein of 110 kD. *Science* **247**, 723–726.
- SARDET, C., FRANCHI, A. AND POUYSSÉGUR, J. (1989). Molecular cloning, primary structure and expression of the human growth factor-activatable Na^+/H^+ antiporter. *Cell* **56**, 271–280.
- SHETLAR, R. E. AND TOWLE, D. W. (1989). Electrogenic sodium-proton exchange in membrane vesicles from crab (*Carcinus maenas*) gill. *Am. J. Physiol.* **257**, R924–R931.
- SIEBERS, D., LEWECK, K., MARKUS, H. AND WINKLER, A. (1982). Sodium regulation in the shore crab *Carcinus maenas* as related to ambient salinity. *Mar. Biol.* **69**, 37–43.
- SIEBERS, D., WILLE, H., LUCU, C. AND VENEZIA, L. D. (1989). Conductive sodium entry in gill cells of the shore crab, *Carcinus maenas*. *Mar. Biol.* **101**, 61–68.
- TAYLOR, H. H. AND TAYLOR, E. W. (1992). Gills and lungs: the exchange of gases and ions. In *Microscopic Anatomy of Invertebrates*, vol. 10, *Decapod Crustacea* (ed. F. W. Harrison and A. G. Humes), pp. 203–293. New York: Wiley-Liss.
- TOWLE, D. W., BAKSINSKI, A., RICHARD, N. E. AND KORDYLEWSKI, M. (1991). Characterization of endogenous Na^+/H^+ antiporter in *Xenopus* oocytes. *J. exp. Biol.* **159**, 359–369.
- TOWLE, D. W. AND KAYS, W. T. (1986). Basolateral localization of Na^+/K^+ -ATPase in gill epithelium of two osmoregulating crabs, *Callinectes sapidus* and *Carcinus maenas*. *J. exp. Zool.* **239**, 311–318.
- TOWLE, D. W., KORDYLEWSKI, M., BOWRING, S. W. AND MORRISON-SHETLAR, A. I. (1992). Molecular biology of the electrogenic sodium/hydrogen antiporter in gills of the green shore crab *Carcinus maenas*. *Bull. Mt Desert Island Biol. Lab.* **31**, 81.
- TSE, C.-M., BRANT, S. R., WALKER, M. S., POUYSSÉGUR, J. AND DONOWITZ, M. (1992). Cloning and sequencing of a rabbit cDNA encoding an intestinal and kidney-specific Na^+/H^+ exchanger isoform (NHE-3). *J. biol. Chem.* **267**, 9340–9346.
- TSE, C. M., MA, A. I., YANG, V. W., WATSON, A. J. M., LEVINE, S., MONTROSE, M. H., POTTER, J., SARDET, C., POUYSSÉGUR, J. AND DONOWITZ, M. (1991). Molecular cloning and expression of a cDNA encoding the rabbit ileal villus cell basolateral membrane Na^+/H^+ exchanger. *EMBO J.* **10**, 1957–1967.
- ZEISKE, W., ONKEN, H., SCHWARZ, H.-J. AND GRASZYNSKI, K. (1992). Invertebrate epithelial Na^+ channels: Amiloride-induced current-noise in crab gill. *Biochim. biophys. Acta* **1105**, 245–252.